

High Rate Copper Electrodeposition in the Presence of Inorganic Salts

H.H. Abdel Rahman, A.H.E. Moustafa*, S.M.K. Abdel Magid

Chemistry Department, Faculty of Science, Alexandria University, Alexandria, Egypt

*E-mail: amirahossameldin@yahoo.com

Received: 29 May 2012 / Accepted: 7 July 2012 / Published: 1 August 2012

Efforts are on increase for finding out the ways to increase electrodeposition rate. This study shows the effect of using different inorganic salts as accelerators for copper electrodeposition. High deposition rate is attributed to enhanced mass transport of copper ions toward the metal surface and lowering the viscosity through the acidic bath using different techniques as potentio-dynamic, rotating cylinder, rotating disk technique. Based on the analysis of the obtained data, the % acceleration for various types of inorganic additives as halides, mono-valent and bi-valent cations increase with increasing additive concentrations and decrease with temperature. Addition of these additives to copper bath exhibits a strong influence on the microstructure of the deposit as shown in the scanning electron microscope analysis. We observe that, in some cases the acceleration behaviour modify the nucleation mechanism and effect on the crystal growth process.

Keywords: Copper; Electrodeposition; Inorganic salts; Acceleration; Scanning electron microscope (SEM).

1. INTRODUCTION

Electrodeposition is one of the key steps in today's for much utilized coating process in industry for many types of applications. Usually, the coatings obtained by electrodeposition present good adherence which is a function of the substrate cleaning treatment [1, 2].

Copper is one of the most typical metals resistant to corrosion. The electrodeposited copper is mainly used in the corrosion and wear resistant coating industry. Cu is regarded as precursors for the production of semiconductor compounds [3]. Electrodeposited copper is used in multilayer coatings, and serves as an under layer before zinc or tin electrodeposition (aiming to alloy them into brass and bronze afterwards). Electrodeposition of copper films has proved to be an effective and less expensive

technology, in comparison to other known techniques i.e. chemical vapour deposition (CVD) and plasma vapour deposition (PVD) [4, 5].

Metals are deposit in a very rough or powdery form, when the electrolysis is carried out at the limiting current. This seems to be a rather general rule in the case of Cu. The possibility of preventing powder formation at the limiting current by means of a suitable additive is a great interest in electroplating and in electrometallurgy in general [6]. The use of these additives leads to considerable improvements in the structural, mechanical and morphological properties of the deposits. In the electroplating baths, various organic and inorganic additives as brighteners are employed [7]. Commonly, the presence of additives in metal plating solutions produces a better levelling effect at the electrodeposited surface as additives distinctly influenced the electrodeposition rate at protrusions and recesses. Additives may also affect the diffusion of reactants from the bulk of the solution towards the reaction front by changing the plating solution properties, and the surface diffusion of metal ad-ions or ad-atoms to stable lattice sites. Furthermore, the preferential adsorption of either additives or their derivatives on the surfaces with diverse curvature may assist the electrodeposition rate. Then, the dominant mechanism of the process might depend on the plating solution composition, the nature of the additives, and the substrate surface morphology [8].

The objective of the present research is mechanistic study the role played by inorganic salts: halides, mono-valent cations and bi-valent cations in improving the Cu deposition rate using different electrochemical techniques. Finally, the deposits obtained in the different conditions were examined with SEM.

2. EXPERIMENTAL

2.1 Materials

Analar grade $\text{CuSO}_4 \cdot 5\text{H}_2\text{O}$ and H_2SO_4 (98% w/w), supplied by BDH Chemicals Ltd., were used for the preparation of the electrolytes. Analar grade of NaCl, LiCl, KCl, NaBr, NaI, MgCl_2 , NiCl_2 , CoCl_2 and MnCl_2 supplied by BDH Chemicals Ltd., were used as inorganic additives.

2.2 Solutions

All solutions were used freshly prepared for each experiment. A concentration of 0.15M CuSO_4 and 1.5M H_2SO_4 (supporting electrolyte) were used in all experiments. Copper sulphate concentration and its content were checked by the iodine thiosulphate method.

2.3 Density and viscosity measurements

The viscosity and density are measured using Stanhope-84100 at 298 ± 1 K. An oscillation period of the measuring cell which is generated when it is given the natural oscillation, will vary depend on the density of the sample in the cell.

2.4 Electrochemical measurements

2.4.1 Potentiodynamic method

The limiting current density was measured using the ordinary cell of two vertical parallel plates, both anode and cathode formed of copper with similar dimensions. The cell consists of a rectangular plastic container ($5.1 \times 5 \times 10 \text{ cm}^3$) with electrodes fitting the whole cross section area. The electrical circuit consists of 6 V D.C. power supply connected in series with the cell and multi-range digital ammeter. A luggin probe is placed where its tip is about 1 mm apart from the bottom one third of the cathode surface. A copper reference electrode is placed in the cup of the luggin probe. A multi-range potentiometer is connected in parallel with the reference electrode and the cathode.

At the beginning, electrodes were mechanically polished with different grades of silicon carbide papers (P150) and washed with distilled water and degreased by acetone. The backs of the cathode and the anode were coated with epoxy resin and also the surface of cathode except an area of ($5 \times 5 \text{ cm}^2$).

Polarization curves, from which the limiting current density was determined were constructed by increasing the current stepwise and measuring the steady state cathode potential against a copper reference electrode. The galvanostatic and the rapid potentiostatic methods gave almost the same limiting current.

2.4.2 The rotating cylinder electrode (RCE) and the rotating disk electrode (RDE)

In case of RCE: the cathode consisted of copper metal cylinder 1 cm diameter, 7cm length and the disk is insulated by epoxy resin. In case of RDE: the cathode consisted of copper metal disk has diameter 1 cm and the cylinder is insulated by epoxy resin. The anode is made of cylindrical copper metal couture electrode of 12 cm diameter; it's also acted as the reference electrode by feature of its high surface area compared to the cathode. Voltmeter is connected in parallel with the cell to measure its voltage.

2.5 Scanning electron microscopy

SEM micrographs of copper electrodeposits prepared from different plating solutions were obtained employing a scanning electron microscope (Cambridge Stereoscan 360 SEM). The electron source was LaB_6 .

Electron detection was carried out with a scintillation photodetector. The typical working pressure was 10^{-7} mbar. The samples were coated with gold by electrodeposition under vacuum prior to analysis. For this purpose electropolished copper sheet cathodes ($1 \text{ cm} \times 1 \text{ cm}$) were used. Before the SEM inspection, each electrode was first rinsed with distilled water, and then with analytical grade acetone.

3. RESULTS AND DISCUSSION

3.1 Electrochemical characterization

Figure 1 shows the cathodic polarization curve for copper electrodeposition from sulphate solution under the influence of increasing NaCl concentrations as example. It is obvious that, in the inorganic free solution, the current at first increases linearly, and then tends to exhibit limiting current plateau with increases in the cathodic potential [6]. Addition of inorganic additives to the sulphate solution decreases the cathodic polarization and increases the value of limiting current density. The observed changes in the cathodic polarization in the presence of inorganic additive suggest that, additives may be acting as an accelerator, which is confirmed by the observation that at any given over potential, the current density for copper deposition from solutions containing inorganic additive is higher than that found for the corresponding inorganic free solution. This acceleration of the rate of the reaction in the presence of inorganic additive on the copper electrodeposition reaction may be due to change in viscosity of solution upon addition of inorganic additives [9].

Experiments data in Table 1 reveal that, as viscosity decrease as convection increase while concentration gradient of inorganic additives increase. This relation between viscosity and convection can be explained in terms of ion mobility (i.e.) as viscosity of solution decreases the solution resistance to the ion moving will decrease and hence the ion mobility will increase and acceleration of the rate of the reaction in the presence of inorganic additive will consequently increase [10, 11]]. Therefore, the limiting current increase as the concentration of inorganic additives increase as predicted in Fig. 1 due to increasing in ion mobility. Values of limiting current for all solutions at different temperatures are given in Table 2. Noticeably, the limiting current increases with increasing inorganic additive concentrations and decreases with temperature [6].

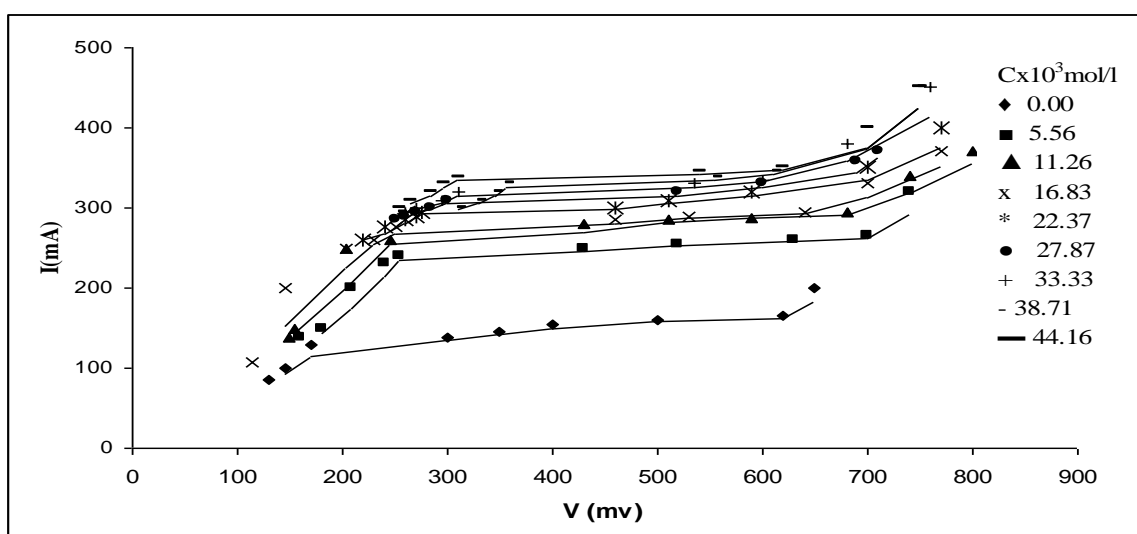


Figure 1. Effect of different concentrations of NaCl mol/l on limiting current (mA) at 298 K.

Table 1. Physical properties η , ρ and D used in calculated dimensionless groups for Cu-Cylinder and Disk of various inorganic additives containing solutions at 298 K.

Inorganic Additives																				
1) NaCl							2) NaBr							3) NaI						
Cx10 ³	i _x x10 ⁻² (Acm ⁻²)	i _x x10 ⁻² (Acm ⁻²)	ρ	η	Dx10 ⁶ (cm ² s ⁻¹)	Dx10 ⁶ (cm ² s ⁻¹)	i _x x10 ⁻² (Acm ⁻²)	i _x x10 ⁻² (Acm ⁻²)	ρ	η	Dx10 ⁶ (cm ² s ⁻¹)	Dx10 ⁶ (cm ² s ⁻¹)	i _x x10 ⁻² (Acm ⁻²)	i _x x10 ⁻² (Acm ⁻²)	ρ	η	Dx10 ⁶ (cm ² s ⁻¹)	Dx10 ⁶ (cm ² s ⁻¹)		
mol/l	Cylinder	Disk			Cylinder	Disk	Cylinder	Disk			Cylinder	Disk	Cylinder	Disk			Cylinder	Disk		
Blank	14.40	8.91	1.0001	1.0284	4.95	7.50	14.40	8.91	1.0001	1.0284	4.95	7.50	14.40	8.91	1.0001	1.0284	4.95	7.50		
5.56	21.19	19.70	0.8120	0.8921	5.46	5.15	20.34	18.40	1.0926	0.9969	4.64	5.00	14.83	17.10	1.0971	1.0146	2.86	4.22		
11.26	22.03	21.00	0.8250	0.8860	5.75	6.00	21.19	19.70	1.0936	0.9886	4.92	5.00	19.49	18.40	1.0981	0.9999	4.34	5.32		
16.83	22.88	22.20	0.8342	0.8740	6.00	6.00	22.03	21.00	1.0952	0.9767	5.19	6.00	19.92	19.70	1.0990	0.9950	4.47	5.00		
22.37	23.31	23.50	0.8417	0.8673	6.12	7.00	22.46	22.20	1.0960	0.9638	5.31	7.00	20.34	21.00	1.0910	0.9910	4.63	6.00		
27.87	23.73	24.80	0.8518	0.8530	6.20	7.00	22.88	23.50	1.0969	0.9554	5.44	7.00	20.76	22.20	1.1012	0.9873	4.74	7.00		
4) LiCl							5) KCl							6) MgCl ₂						
Blank	14.40	8.91	1.0001	1.0284	4.95	7.50	14.40	8.91	1.0001	1.0284	4.95	7.50	14.40	8.91	1.0001	1.0284	4.95	7.50		
5.56	26.70	22.20	0.7236	0.7015	7.31	6.00	16.95	12.70	1.0458	1.0310	3.90	3.00	16.95	20.37	1.0874	0.9231	4.70	6.00		
11.26	27.54	23.50	0.7241	0.6976	7.65	7.00	17.80	14.00	1.0479	1.0279	3.90	3.00	17.37	21.64	1.0882	0.9143	3.40	6.00		
16.83	27.97	24.80	0.7262	0.6910	7.79	8.00	18.64	15.20	1.0482	1.0231	4.20	4.00	17.80	22.91	1.0895	0.9063	3.50	7.26		
22.37	28.39	26.10	0.7269	0.6853	7.93	8.00	19.07	16.50	1.0491	0.9831	4.30	4.00	18.22	24.19	1.0900	0.8931	3.60	8.00		
27.87	28.81	27.30	0.7278	0.6815	8.08	9.00	19.42	17.80	1.0504	0.9730	4.40	5.00	18.64	25.46	1.0916	0.8868	3.70	8.00		
7) NiCl ₂							8) CoCl ₂							9) MnCl ₂						
Blank	14.40	8.91	1.0001	1.0284	4.95	7.50	14.40	8.91	1.0001	1.0284	4.95	7.50	14.40	8.91	1.0001	1.0284	4.95	7.50		
5.56	16.10	11.45	1.0927	0.9689	3.70	2.05	15.68	8.91	1.0915	1.1001	3.80	2.02	14.83	7.63	1.0938	1.1150	3.60	1.11		
11.26	16.53	12.73	1.0930	0.9540	3.20	3.02	15.68	10.18	1.0901	0.9963	3.30	2.26	15.25	8.91	1.0940	0.9998	3.00	2.09		
16.83	16.95	14.00	1.0935	0.9460	3.30	3.08	16.53	11.45	1.0918	0.9879	3.10	2.22	15.68	10.18	1.0956	0.9985	3.00	2.15		
22.37	17.37	15.27	1.0937	0.9376	3.40	4.03	16.95	12.73	1.0921	0.9731	3.30	3.09	16.10	11.45	1.0960	0.9863	3.10	9.00		
27.87	18.22	16.55	1.0939	0.9261	3.50	4.12	17.37	14.00	1.0936	0.9636	3.50	3.20	16.53	12.73	1.0969	0.9750	3.20	3.00		

3.2 Effect of inorganic additives on the Limiting Current

Among several techniques to augment the mass transfer coefficients; using different inorganic additives which have ability for accelerating copper electrodeposition as shown in Table 2.

The percentage acceleration can be calculated according to the following equation [6]:

$$\% \text{Acceleration} = \frac{(I)_{\text{inorg.}} - (I)_{\text{blank}}}{(I)_{\text{blank}}} \times 100 \quad (1)$$

where $(I)_{\text{blank}}$, $(I)_{\text{inorg}}$ are the limiting current in absence and in presence of inorganic additives respectively. Those additives have an accelerating effect on the kinetics of the copper discharge process, pointed out by the increase of the limiting current. The observed enhancement in the rate of Cu deposition in presence of increasing concentration of inorganic additives may be due to:

a) A decrease in viscosity that was found experimentally upon concentration gradient of inorganic additives which by it's role depends on ion transport that increase by decreasing in viscosity [10], therefore the mass transfer coefficient will increase and the rate of electrodeposition increases.

b) The presence of inorganic additive changes the mechanism of the copper electrodeposition as it can be seen from increasing the cathodic mass transfer coefficient. A possible explanation for this fact consists in the increasing role of an additional reaction that produces the same chemical species (Cu^+) as those involved in the rate determining reaction [12].

Figure 2 and Table 2 show the percentage acceleration caused by using different types of inorganic additives for Cu electrodeposition at different temperatures which ranging from 0.91% to

150% for halides, 18.18% to 158.70% for mono-valent cations and from 31.82 to 131.88 for bi-valent cations.

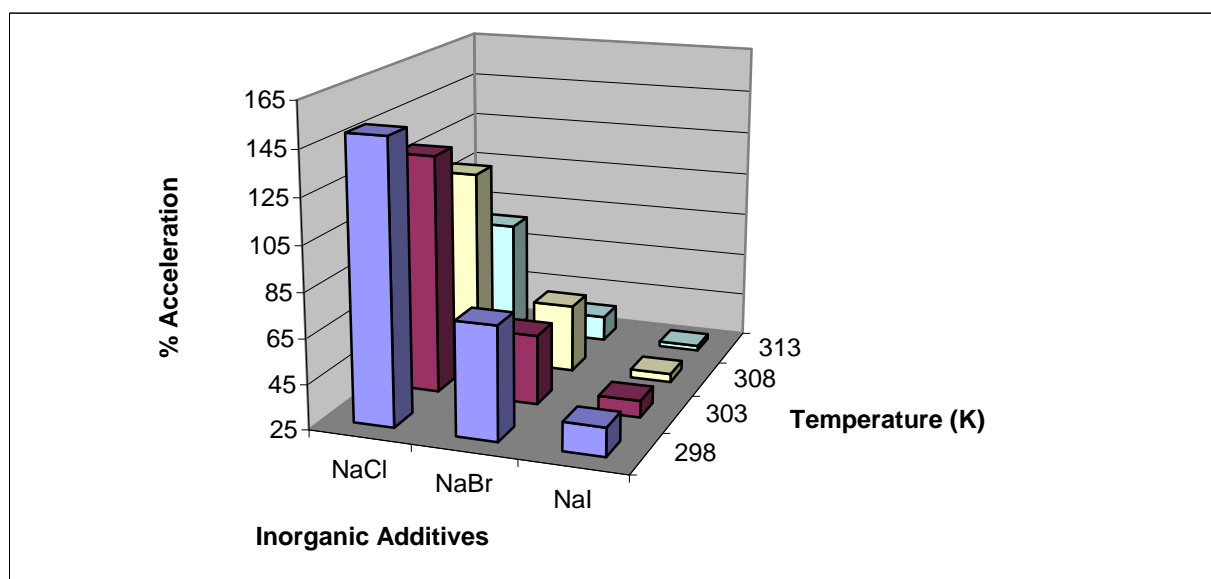


Figure 2. Variation of % acceleration for copper electrodeposition using different inorganic additives at concentration 44.16×10^{-3} mol/l at different temperature.

3.3 Effect of Electrode Rotation (Forced Convection)

In this work, the electrodeposition of copper in the presence of inorganic additives is investigated using rotating disk electrode (RDE) and rotating cylinder electrode (RCE) techniques. The rotating electrodes are hydrodynamic tools that use forced convection to enhance the mass transport rate to the electrode surface. The control of convective diffusion by electrode rotation enables quantitative studies of metal deposition. The RDE is used to provide information on the electrodeposition mechanism, under controlled laminar flow conditions. On the other hand, the RCE normally generates turbulent flow and provides a uniform current distribution along the cathode [13, 14]. The effect of the speed of rotation on the rate of metal deposition can also be used to determine whether the electrodeposition process is diffusion or chemically controlled process. Our data as shown in Fig. 3(a) and (b), give the relation between the limiting current density and the angular velocity, $\omega = \frac{2\pi rpm}{60}$, to the power 0.7 for RCE and to the power 0.5 for RDE at 298 K and different concentrations of inorganic additive used. Straight lines were obtained and the limiting current density increases by increasing the rotation speed which indicates that electrodeposition process of copper is diffusion controlled reaction.

Table 2. Values of limiting current and % acceleration for all inorganic additives at different temperatures.

Inorganic Additives	Cx10 ³ mol/l	298 K		303 K		308 K		313 K	
		I _l (mA)	%Acc.	I _l (mA)	%Acc.	I _l (mA)	%Acc.	I _l (mA)	%Acc.
1)NaCl	Blank	138	0	160	0	180	0	220	0
	5.56	250	81.16	285	78.13	290	61.11	300	36.36
	11.26	276	100.00	316	97.50	320	77.78	325	47.73
	16.83	285	106.52	325	103.13	330	83.33	335	52.27
	22.37	300	117.39	340	112.50	348	93.33	355	61.36
	27.87	320	131.88	348	117.50	355	97.22	359	63.18
	33.33	330	139.13	355	121.88	365	102.78	368	67.27
	38.76	339	145.65	365	128.13	379	110.56	381	73.18
2) Na Br	44.16	345	150.00	371	131.88	384	113.33	390	77.27
	5.56	155	12.32	170	6.25	190	5.56	230	4.55
	11.26	173	25.36	180	12.50	200	11.11	240	9.09
	16.83	185	34.06	190	18.75	221	22.78	250	13.64
	22.37	195	41.30	200	25.00	224	24.44	260	18.18
	27.87	212	53.62	215	34.38	235	30.56	270	22.73
	33.33	230	66.67	231	44.38	250	38.89	280	27.27
	38.76	238	72.46	245	53.13	260	44.44	290	31.82
3)Na I	44.16	242	75.36	250	56.25	280	55.56	300	36.36
	5.56	140	1.45	162	1.25	182	1.11	222	0.91
	11.26	145	5.07	168	5.00	188	4.44	227	3.18
	16.83	150	8.70	172	7.50	192	6.67	233	5.91
	22.37	155	12.32	179	11.88	199	10.56	241	9.55
	27.87	165	19.57	185	15.63	207	15.00	250	13.64
	33.33	170	23.19	192	20.00	215	19.44	260	18.18
	38.76	180	30.43	202	26.25	222	23.33	270	22.73
4) LiCl	44.16	190	37.68	212	32.50	232	28.89	280	27.27
	5.56	260	88.41	290	81.25	300	66.67	310	40.91
	11.26	280	102.90	320	100.00	330	83.33	340	35.29
	16.83	290	110.14	332	107.50	340	88.89	345	36.23
	22.37	310	124.64	349	118.13	350	94.44	355	38.03
	27.87	330	139.13	358	123.75	365	102.78	368	40.22
	33.33	340	146.38	365	128.13	374	107.78	380	42.11
	38.76	350	153.62	371	131.88	385	113.89	391	43.73
5)Kcl	44.16	357	158.70	380	137.50	391	117.22	400	45.00
	5.56	230	66.67	240	50.00	250	38.89	260	18.18
	11.26	258	86.96	263	64.38	265	47.22	270	22.73
	16.83	270	95.65	278	73.75	280	55.56	285	29.55
	22.37	285	106.52	299	86.88	305	69.44	310	40.91
	27.87	299	116.67	312	95.00	320	77.78	325	47.73
	33.33	310	124.64	330	106.25	335	86.11	340	54.55
	38.76	321	132.61	345	115.63	350	94.44	355	61.36
6)MgCl ₂	44.16	330	139.13	360	125.00	365	102.78	370	68.18
	5.56	250	81.16	260	62.50	290	61.11	330	50.00
	11.26	260	88.41	270	68.75	300	66.67	340	54.55
	16.83	270	95.65	280	75.00	310	72.22	350	59.09
	22.37	280	102.90	290	81.25	320	77.78	360	63.64
	27.87	290	110.14	300	87.50	330	83.33	370	68.18
	33.33	300	117.39	310	93.75	340	88.89	380	72.73
	38.76	310	124.64	320	100.00	350	94.44	390	77.27
7)NiCl ₂	44.16	320	131.88	330	106.25	360	100.00	400	81.82
	5.56	230	66.67	240	50.00	270	50.00	310	40.91
	11.26	240	73.91	250	56.25	280	55.56	320	45.45
	16.83	250	81.16	260	62.50	290	61.11	330	50.00
	22.37	260	88.41	270	68.75	300	66.67	340	54.55
	27.87	270	95.65	280	75.00	310	72.22	350	59.09
	33.33	280	102.90	290	81.25	320	77.78	360	63.64
	38.76	290	110.14	300	87.50	330	83.33	370	68.18
8)CoCl ₂	44.16	300	117.39	310	93.75	340	88.89	380	72.73
	5.56	220	59.42	230	43.75	260	44.44	300	36.36
	11.26	230	66.67	240	50.00	270	50.00	310	40.91
	16.83	240	73.91	250	56.25	280	55.56	320	45.45
	22.37	250	81.16	260	62.50	290	61.11	330	50.00
	27.87	260	88.41	270	68.75	300	66.67	340	54.55
	33.33	270	95.65	280	75.00	310	72.22	350	59.09
	38.76	280	102.90	290	81.25	320	77.78	360	63.64
9)MnCl ₂	44.16	290	110.14	300	87.50	330	83.33	370	68.18
	5.56	210	52.17	220	37.50	250	38.89	290	31.82
	11.26	220	59.42	230	43.75	260	44.44	300	36.36
	16.83	230	66.67	240	50.00	270	50.00	310	40.91
	22.37	240	73.91	250	56.25	280	55.56	320	45.45
	27.87	250	81.16	260	62.50	290	61.11	330	50.00
	33.33	260	88.41	270	68.75	300	66.67	340	54.55
	38.76	270	95.65	280	75.00	310	72.22	350	59.09
	44.16	280	102.90	290	81.25	320	77.78	360	63.64

The diffusion coefficient; D , in case of RCE, was determined from the limiting current density as shown in Table 1, using Eisenberg equation [15]

$$I_L = knFC_b d^{0.3} v^{-0.344} D^{0.644} U^x \quad (2)$$

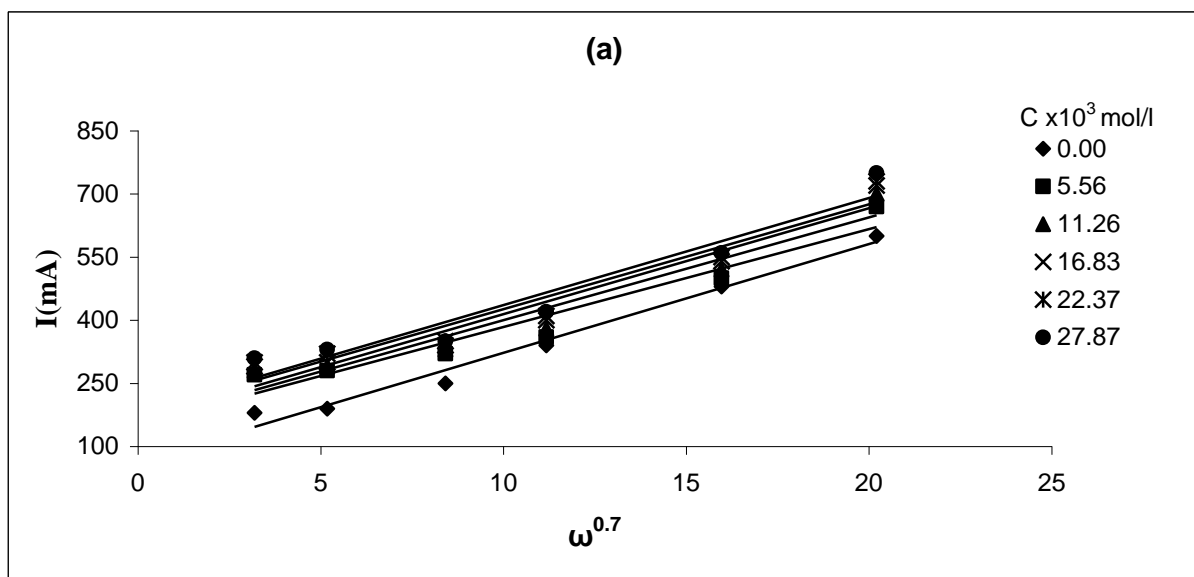
where $k = 0.0971$ and $x = 0.7$, n is the number of electrons involved in process, F is Faraday's constant ($A \ s \ mol^{-1}$), C_b is the bulk concentration ($mol \ cm^{-3}$), U is the electrode peripheric velocity = ωr in $cm \ rad \ s^{-1}$ (r is the radial distance in cm), d is the characteristic length of the rotating cylinder in cm , D is the diffusion coefficient for the metal ions in $cm^2 \ s^{-1}$, and v is the kinematics viscosity ($v = \eta/\rho$) where η is viscosity in poise and ρ is density $g \ cm^{-3}$ [16]. It was observed that the values of D for Cu^{2+} ions in solutions containing inorganic additives increases due to decrease in interfacial viscosity (η) in accordance with the Stokes-Einstein equation [17]:

$$\frac{\eta D}{T} = const. \quad (3)$$

The Levich equation for RDE may be applied to relate the limiting current density j_{mt} to the electrode rotating rate ω

$$j_{mt} = 0.620 F D_{obs}^{2/3} \omega^{1/2} v^{-1/6} C_{red,b} \quad (4)$$

where D_{obs} is an observed diffusion coefficient, v is kinematics viscosity, and $C_{red,b}$ is the bulk concentration of the reduced species. The slight increase of D values observed in the presence of additives indicates that additives help the diffusion of cupric ions from the bulk solution to the outer limit of the electrode double layer.



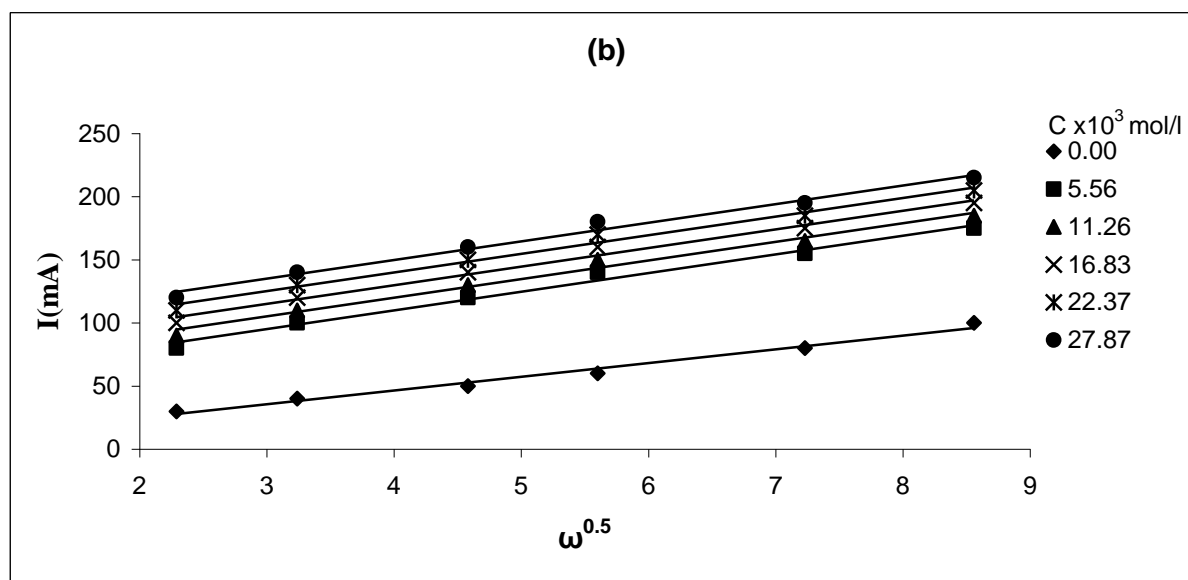


Figure 3. The relation between i_L and (a) $\omega^{0.7}$ for cylinder, (b) $\omega^{0.5}$ for disk at 298K for NaCl.

A possible explanation is that inorganic additives are polar molecules with interfacial activity, which could change the composition and the properties of the double layer on the electrode surface. Thus, the additives molecules replace the water molecules on the metallic surface, forming an adsorbed superficial film. This would decrease the electrolyte viscosity and increase the dielectric constant at the electrode interface. Consequently, hydrated metal ions approach the surface with increased difficulty to enable charge transfer [16].

3.4 Mass transport characterization at RCE and RDE

RCE and RDE are particularly well suited for high mass transport studies in the turbulent and laminar flow regime. When the fluid flow is generated entirely by an inner RCE and RDE, the characteristics of mass transport conditions can be described by a dimensionless group correlation of the following form:

$$Sh = a Re^c Sc^b \quad (5)$$

where the Sherwood number ($Sh = kL/D$) describes mass transport by forced convection, the Reynolds number ($Re = dU/\nu$) is an indication of the fluid flow regime, and the Schmidt number ($Sc = \nu/D$) relates the electrolyte transport properties. The average mass transport coefficient is k , cm s^{-1} ($k = i_L/zFC_{Cu^{2+}}$ where i_L is the limiting current density, $C_{Cu^{2+}}$ is saturation solubility of copper sulphate, z is the valance, F is Faraday's constant in A s mol^{-1}), L is length of cylinder, cm , D is the diffusion coefficient, $\text{cm}^2 \text{s}^{-1}$, ν is kinematics viscosity, $\text{cm}^2 \text{s}^{-1}$ and U is rotation velocity $= \omega r$, cm s^{-1} , d is the diameter of the cylinder in cm . The experimental constant a , is associated with the electrode geometry, shape, cell dimensions as well as with the diffusion coefficient whereas b is associated with the

hydrodynamic regime and $c = 0.33$ indicating forced convection regime [18, 19]. By plotting $\log \text{Sh}/(\text{Sc})^{0.33}$ against $\log \text{Re}$, a straight line was obtained its slope gave the constant "b" while the intercept gives the constant "a". Figure 4 (a) and (b) give the over all correlation for all inorganic additives used can give by the following equation:

$$\text{Sh} = 0.238 \text{Re}^{0.72} \text{Sc}^{0.33} \quad \text{for RCE} \quad (6)$$

In case of RCE a forced convection mechanism is obtained which agree very well with similar relationships reported before [15, 20].

$$\text{Sh} = 0.358 \text{Re}^{0.50} \text{Sc}^{0.33} \quad \text{for RDE} \quad (7)$$

In case of RDE a laminar convection mechanism is obtained which agree very well with similar relationships reported before [21, 22].

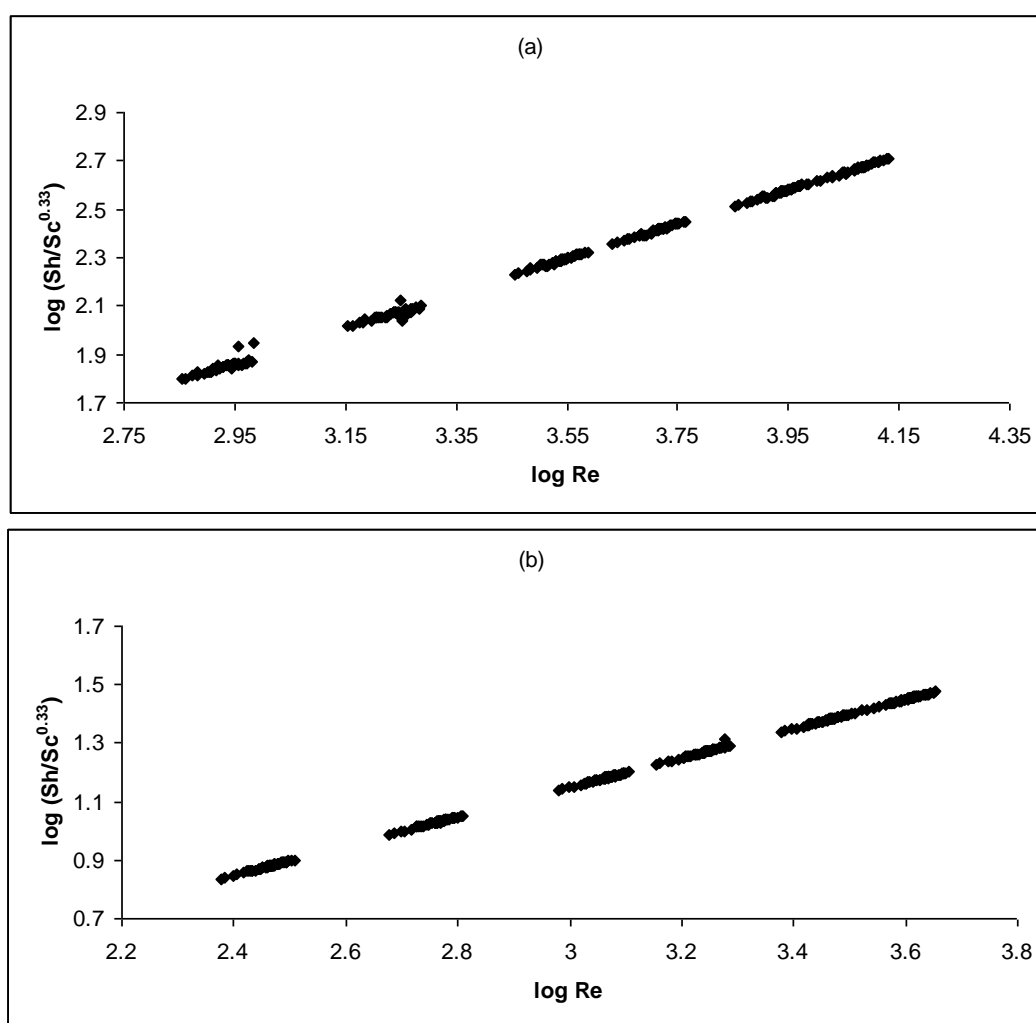


Figure 4. The overall correlation for all inorganic additives in case of Cu (a) cylinder and (b) disk at 298 K.

3.5 Effect of temperature and thermodynamic parameters

The electrodeposition of copper in presence of different inorganic additives was studied by measuring the limiting current over the temperature range of 298 - 313 K. It can be seen in Table 1 that the limiting current and % acceleration for all compounds decrease with increasing temperature. The electrodeposition process can be regarded as an Arrhenius-type process. The activation parameters for the studied systems were calculated from Arrhenius equation [23]. From Table 3, calculated activation energies are ranged from 7.69 to 38.40 kJ mol⁻¹ for the electrodeposition process in the absence and presence of inorganic additives. The increasing activation energies in the presence of accelerators indicate that physical adsorption (electrostatic) occurs and diffusion controlled adsorption in the first stage [24]. For example, in the case of halides, NaCl in which the deposition rate increases rapidly with temperature, the E_a values are higher. With the other two additives (NaBr, NaI) the E_a values are lower than NaCl but higher than blank. The higher activation energies mean that the reaction rate is very sensitive to temperature. The very high E_a values in the case of NaCl also suggest that the adsorption of the additive on the metal surface may be physical or weak in nature but in case of NaBr or NaI suggest the lower rate of gas evolution [25].

In this research, the thermodynamic parameters such as the enthalpy (ΔH^*), the entropy change (ΔS^*) and the free energy change of the adsorption (ΔG^*) were calculated in same way as the related researches did in literature [26]. Table 3 summarizes the values of these thermodynamic properties. The results show positive sign for ΔH^* , reflecting the endothermic nature of the electrodeposition process. The negative values of (ΔS^*) pointed to greater order produced during the process of activation and non- random distribution of ions [23]. ΔG^* values show limited increase with rise in the concentration of inorganic additives i.e ΔG^* values of the accelerated systems were more positive than that for the blank revealing the weak dependence of (ΔG^*) on the composition of inorganic additives. In all cases (ΔH^*) and (ΔS^*) compensate each other to produce little change in (ΔG^*) [24].

By plotting ΔH^* versus ΔS^* for all amines compound, this correlation can be treated as isokinetic relationship, where the slope β represents the isokinetic temperature. The temperatures will be 759, 531, 803, 812, 685, 363, 428, 366 and 352 K for NaCl, LiCl, KCl, NaBr, NaI, MgCl₂, NiCl₂, CoCl₂ and MnCl₂, respectively, which is much higher than the experimental temperature. This indicates that the electrodeposition reaction is under activation- control, where the addition of the studied inorganic additives playing an important role in accelerating the electrodeposition rate but without changing the electrodeposition mechanism as indicated by the observed parallelism between (ΔH^*) and (ΔS^*) [5, 23].

3.6 Structure effect of inorganic additives

Halides have been reported to accelerate the deposition of some metals in strong acids and this effect depends on the ionic size, charge, the electrostatic field setup by the negative charge of the anion on adsorption sites and the nature and concentration of halide ions. Many attempts had been made to explain the difference in the action of the halides which may depend on the atomic radii.

- For series of NaCl, NaBr, NaI the order of increasing rate of deposition reaction is: NaCl > NaBr > NaI.

Table 3. Electrodeposition Thermodynamic parameters in the presence of different inorganic additives.

Inorganic Additives	Cx10 ³ mol/l	E _a (kJ mol ⁻¹)	ΔH* (kJ mol ⁻¹)	ΔS* (Jmol ⁻¹ K ⁻¹)	ΔG* (kJ mol ⁻¹)	Inorganic Additives	E _a (kJ mol ⁻¹)	ΔH* (kJ mol ⁻¹)	ΔS* (Jmol ⁻¹ K ⁻¹)	ΔG* (kJ mol ⁻¹)	Inorganic Additives	E _a (kJ mol ⁻¹)	ΔH* (kJ mol ⁻¹)	ΔS* (Jmol ⁻¹ K ⁻¹)	ΔG* (kJ mol ⁻¹)
1) NaCl	Blank	7.69	7.21	-202.00	67.63	4) LiCl	7.69	7.21	-202.00	67.63	7) NiCl ₂	7.69	7.21	-202	67.63
	5.56	21.56	19.08	-185.48	74.38		23.31	20.83	-182.97	75.38		12.40	9.92	-203.00	70.22
	11.26	21.83	19.35	-182.20	75.07		25.65	25.60	-179.16	76.65		12.81	10.33	-201.00	70.31
	16.83	22.34	19.86	-180.19	75.50		28.30	28.73	-175.23	77.71		13.42	10.94	-200.00	70.47
	22.37	22.67	20.19	-175.36	75.98		30.62	30.63	-173.92	78.83		16.00	13.52	-194.00	71.21
	27.87	33.26	30.78	-170.61	81.65		34.55	32.07	-170.15	79.95		16.17	13.67	-194.00	71.40
	33.33	35.66	33.18	-167.56	81.94		36.65	34.17	-168.91	82.21		17.14	14.66	-190.00	72.30
	38.76	35.97	34.66	-165.52	82.20		37.54	35.06	-167.32	83.36		19.22	16.74	-184.00	72.60
2) NaBr	44.16	37.04	35.85	-162.58	83.91	5) KCl	38.40	35.22	-166.81	85.50	8) CoCl ₂	20.70	18.22	-186.00	73.14
	Blank	7.69	7.21	-202.00	67.63		7.69	7.21	-202.00	67.63		7.69	7.21	-202.00	67.63
	5.56	10.86	8.39	-200.67	68.22		19.93	15.56	-192.56	80.32		12.82	10.39	-201.00	70.17
	11.26	12.03	9.55	-198.16	68.82		22.31	16.59	-189.51	81.20		13.22	10.70	-201.00	70.40
	16.83	12.68	10.21	-197.36	69.29		24.63	17.22	-187.23	82.05		13.33	10.75	-200.00	70.98
	22.37	13.30	10.82	-194.12	69.66		27.73	18.23	-185.39	83.29		14.39	11.19	-196.00	71.20
	27.87	15.30	12.82	-189.33	70.70		29.31	19.98	-184.31	84.16		14.71	12.23	-196.00	71.65
	33.33	18.24	15.76	-186.97	72.21		31.01	20.16	-182.65	85.21		15.16	12.69	-194.00	71.86
3) NaI	38.76	19.87	17.39	-183.12	73.13	6) MgCl ₂	32.16	21.95	-181.15	86.11	9) MnCl ₂	17.00	14.52	-190.00	71.85
	44.16	20.03	19.31	-180.15	74.15		33.28	23.31	-180.50	87.20		17.74	15.26	-188.00	71.99
	Blank	7.69	7.21	-202.00	67.63		7.69	7.21	-202.00	67.63		7.69	7.21	-202	67.63
	5.56	9.77	7.40	-201.50	67.69		10.72	11.99	-195.67	71.21		14.62	12.15	-196.00	70.57
	11.26	10.09	7.49	-201.00	67.86		10.89	12.78	-195.23	71.30		15.09	12.62	-195.00	70.71
	16.83	10.26	7.66	-200.50	67.95		11.50	13.93	-192.75	71.68		15.69	13.29	-194.00	70.78
	22.37	10.41	7.78	-200.00	68.03		12.01	14.37	-192.32	72.14		15.79	13.39	-193.00	70.96
	27.87	10.71	7.88	-199.50	68.28		12.36	15.84	-191.82	72.53		15.77	13.42	-192.00	71.50
	33.33	10.82	7.99	-199.00	68.31		12.64	16.12	-189.21	73.79		16.77	14.57	-191.00	71.69
	38.76	10.96	8.23	-198.50	68.50		12.88	17.36	-186.55	73.97		17.05	14.68	-191.00	71.83
	44.16	11.01	8.41	-198.00	68.87		14.30	18.77	-186.81	74.25		17.40	14.92	-189.00	71.94

The increase in rate of deposition reaction is explained on the basis that electro-negativity decreases from Cl⁻ to I⁻ (Cl⁻ = 3.0, Br⁻ = 2.8, I⁻ = 2.5) [27]. It has been reported that the acceleration effect of halides increases in the order I⁻ < Br⁻ < Cl⁻, which seems to indicate that the radii of halogen atoms may have an important role to play. The iodide ion radius (135pm) is more predisposed to adsorption than the bromide ion (114pm) and the chloride ion (90pm).

- For series of mono-valent cations LiCl, NaCl, KCl the order of increasing the rate of deposition reaction is: LiCl > NaCl > KCl, that is due to the potassium atom has high steric hindrance than Na or Li atoms which have less atomic size [27].

• For series of bi-valent cations the order of increasing the rate of deposition reaction is MgCl₂ > NiCl₂ > CoCl₂ > MnCl₂, This is explained on the basis that the reversible potential decrease from Mn (E_{r,Mn} = -1.185) to Mg (E_{r,Mg} = -0.2372) i.e the higher % acceleration value may be due to lower reversible potential [28] and all of the above has been shown in Fig. 5.

3.7. SEM analysis of the deposits

At the conclusion of the electrodeposition process, performed on copper electrode in the presence and absence of inorganic additives, the copper deposits were studied by SEM analysis. It can be noted that the surface morphology was markedly affected by the nature of the inorganic additives. The surface morphology of copper samples immersed in a bath of 0.15M $\text{CuSO}_4 \cdot 5\text{H}_2\text{O}$, 1.5M H_2SO_4 with or without additives has widely studied. All experiments were made at the limiting current density determined for all solutions at 298 K and time of 5 minutes. The analysis of copper morphology shown in Fig. 6 (a) after 5 minutes in absence of inorganic additives reveals less uniform and slightly roughness of the entire electrode surface [29-31]. Figure 6 (b, c, d) give the morphology of the electrodeposited copper in presence of inorganic additives as halides NaCl, NaBr and NaI respectively.

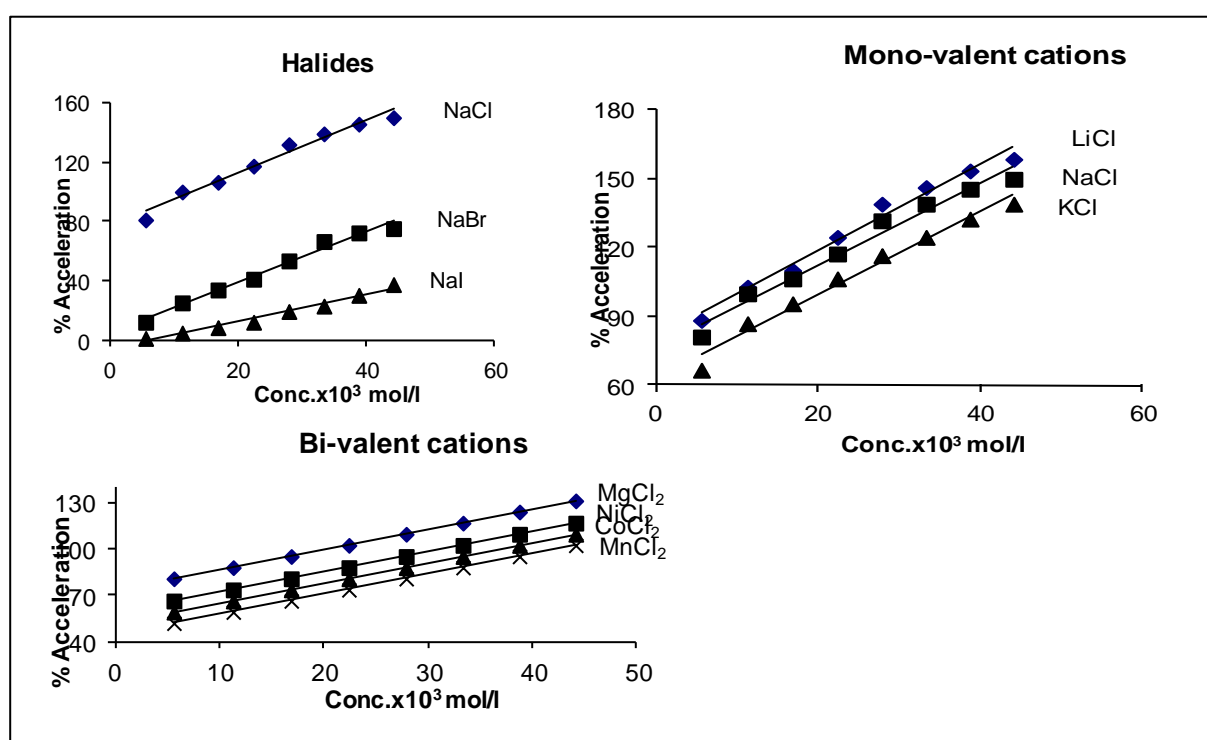


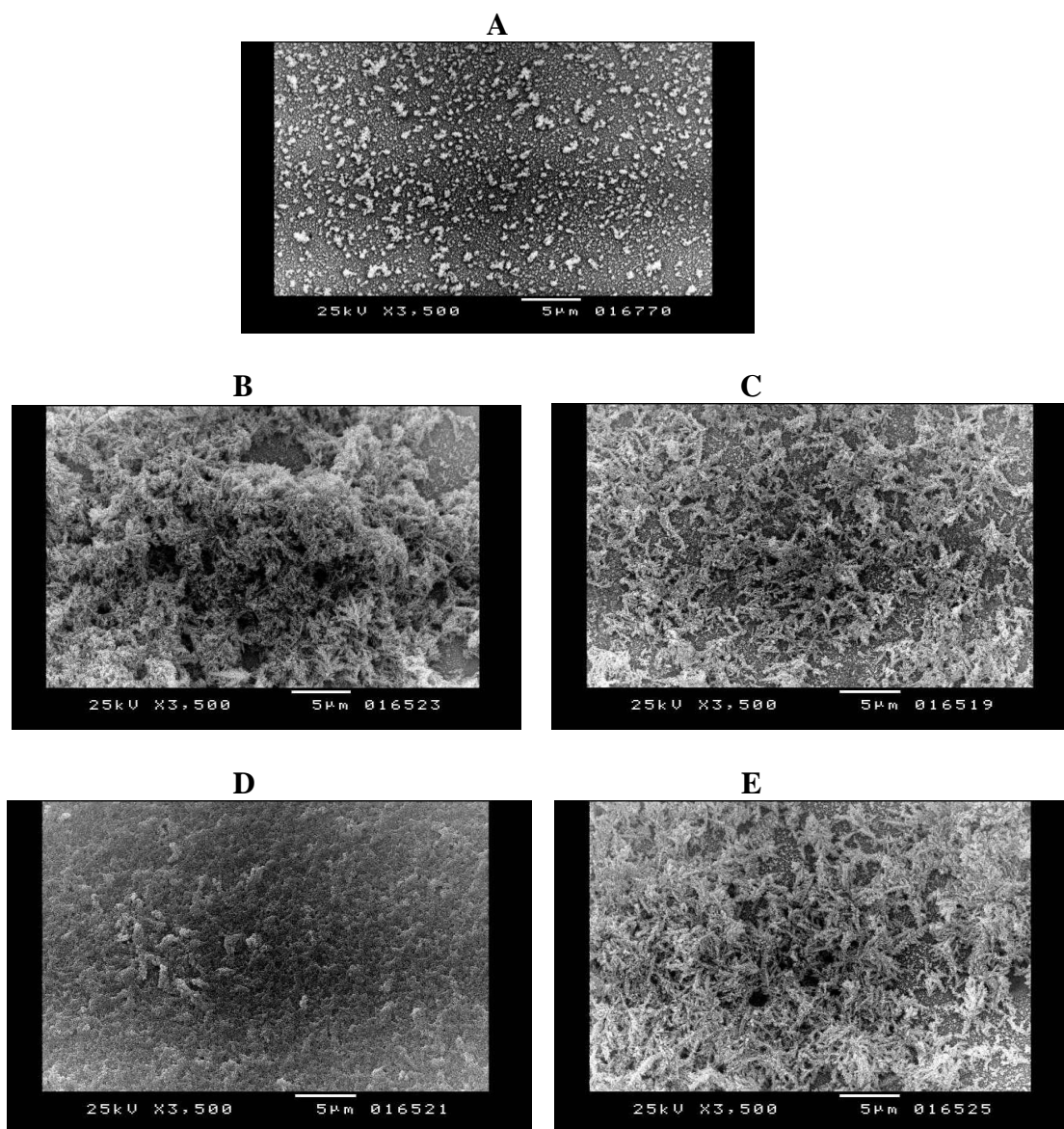
Figure 5. The relation between % acceleration and concentration (mol/l) for inorganic additives at 298 K.

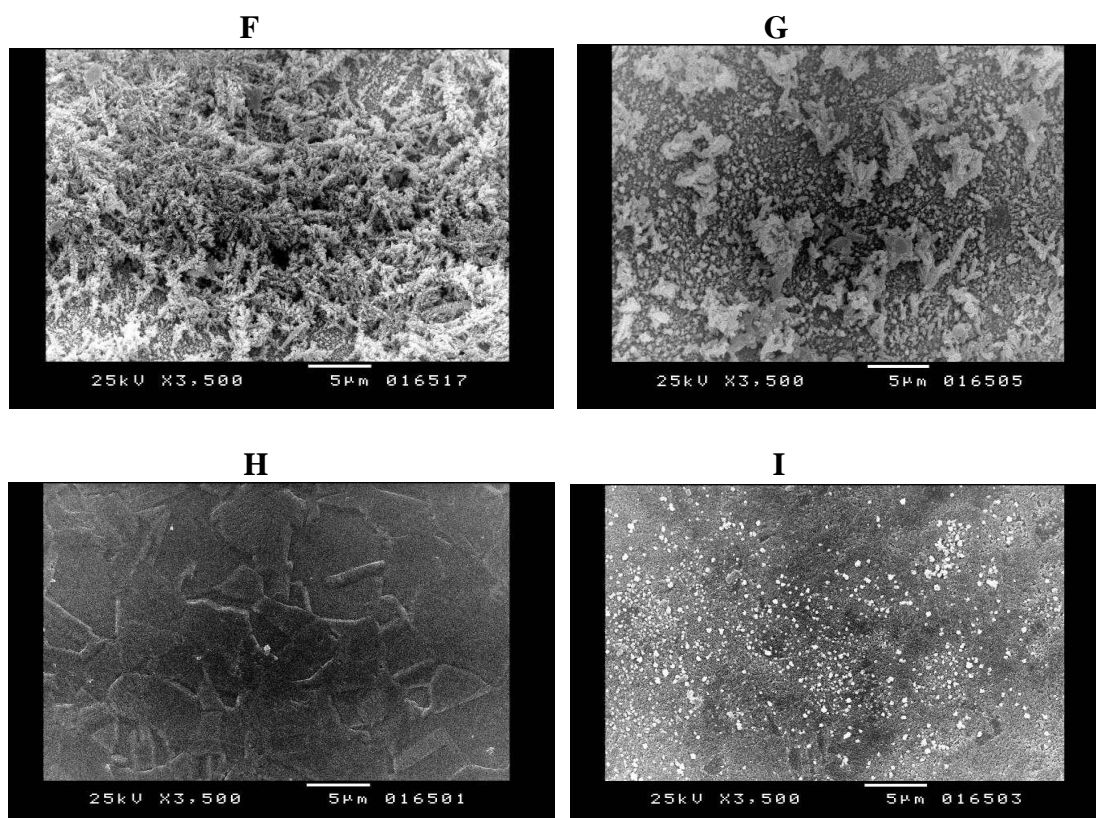
In case of NaCl and NaBr, the copper particles were highly branched dendrites. According to Wranglen, a dendrite consists of branches. This shape is obviously caused by the vigorous hydrogen evolution, or hydrogen stream, which prevents the growth of the copper deposit in one direction, resulting in particles with a curvilinear form and give rougher layer [32-34]. The typical copper dendrite structures have been explained on the basis of diffusion limited aggregation (DLA) model, because the poly-crystalline copper branches are a typical characteristic of DLA-like copper deposits [35-37], so the electrodeposition process which led to formation of highly branched dendrites particles was controlled by diffusion of ions to the electrode surface, rather than electron transfer control [32,

33, 38]. But in case of NaI, the deposit was dense, adherent, smooth, homogenous and the surface coverage was quite satisfactory i.e: increasing corrosion resistance and refining the deposit because it modifies the nucleation mechanism and inhibits crystal growth process [39-42] so the order of acceleration is $\text{NaCl} > \text{NaBr} > \text{NaI}$.

Figure 6 (b, e) comparing the deposit morphologies by using different concentrations of NaCl ($16.83 \times 10^3 \text{ M}$, $33.33 \times 10^3 \text{ M}$) so, as the NaCl content increases the coating surfaces become increasingly in homogeneous with appearance of coarser granular features. The surface roughness of composite coatings increases with increasing NaCl concentration [43].

Figure 6 (b, f-i) show SEM images for copper electrodeposits in presence of (NaCl , KCl , MgCl_2 , NiCl_2 , CoCl_2) respectively .It can be seen from these Figures that the change of cations reveal a highly changes of the surface morphology. Some cations in copper bath acts as a grain refiner that the grains become smaller and deposit was dense, adherent and slightly roughness in some cases and smooth homogeneous in other cases [29-31, 40, 41, 44].





According to the order of acceleration $\text{NaCl} > \text{KCl} \& \text{MgCl}_2 > \text{NiCl}_2 > \text{CoCl}_2$, we can conclude that as acceleration decreases the nucleation mechanism modify and inhibit crystal growth process [39-42].

4. CONCLUSION

- The presence of inorganic additives in the copper bath had a major positive effect on the deposition rate.
- The values of % acceleration increases with increasing accelerator concentrations and decreases with temperatures.
- The activation energy values in the presence of accelerators are higher than that for blank solutions indicating physical mechanism of adsorption.
- By increasing speed of rotation, the reaction rate increases, this indicates that the reaction is diffusion control.
- Addition of these inorganic additives to copper bath exhibits a strong influence on the feature of deposited surface. In some cases give highly branched dendrites as acceleration increased and dense, adherent and slightly roughness deposit in case of low acceleration.

References

1. N.T.M. Hai, T.T. M. Huynh, A. Fluegel, D. Mayer, W. Reckien, T. Bredow, P. Broeckmann, *Electrochim. Acta*, (2012) in press.
2. C.V. Pecequilo, Z. Panossian, *Electrochim. Acta*, 55 (2010) 387.
3. I.B. Assaker, M. Dhahbi, *J. Molec. Liq.*, 161 (2011) 13.
4. P.V. Dudin, O.V. Reva, T.N. Vorobyova, *Surf. Coat. Technol.*, 204 (2010) 3141.
5. H.H. Abdel-Rahman, A.A. Harfoush, A.H.E. Moustafa, *Electrochemistry*, 80 (2012) 226.
6. A.N. Murashkevich, I.M. Zharskij, Kremnij-soderzhachie produkty kompleksnoj pererabotki fosfatnogo syrja, BGTU, Minsk, 2002.
7. M. Hosseini, S. Ebahimi, *J. Electroanal. Chem.*, 645 (2010) 109.
8. M.A. Pasquale, L.M. Gassa, A.J. Ariva, *Electrochim. Acta*, 53 (2008) 5891.
9. E. Mattsson, J.O'M. Bockris, *Trans. Faraday Soc.*, 55 (1959) 1586.
10. S.G. Grinbank, G.D. Costanzo, A. Soba, G.A. Gonzalez, G. Marshall, *J. Electrostat.*, 67 (2009) 672.
11. H.M.A. Soliman, *Appl. Surf. Science*, 195 (2002) 155.
12. T.C. Franklin, *Plat Surf. Finish*, 4 (1994) 62.
13. A. Rec'endiz, I. Gonz'alez, J.L. Nava, *Electrochim. Acta.*, 52 (2007) 6880.
14. C.T.J. Low, F.C. Walsh, *Surf. Coat. Technol.*, 202 (2008) 1339.
15. M. Eisenberg, C. W. Tobias, and C. R. Wilke, *J. Electrochem. Soc.*, 101 (1954) 306.
16. G. Kear, B.D. Barker, K.R. Stokes, F.C. Walsh, *Electrochim. Acta*, 52 (2007) 1889.
17. G.M. El-Subruti, A.M. Ahmed, *Portugaliae Electro Chim. Acta*, 20 (2002) 15.
18. A. Rec'endiza, S. Le'nb, J. L. Navac, F. F. Rivera, *Electrochim. Acta*, 56 (2011) 1455.
19. D.R. Gabe and F.C. Walsh, *J. App. Electrochem.*, 13 (1983) 3.
20. H.H. Abdel-Rahman, *J. Dispersion. Sci. Technol.*, 31 (2010) 1740.
21. V.G. Levich, Physicochemical. Hydrodynamics, Prentice-Hall, Inc., Englewood Cliffs, NJ, USA, (1962).
22. G. Kear, B.D. Barker, K.R. Stokes, F.C. Walsh, *Electrochim. Acta*, 52 (2007) 1889.
23. E.A. Noor, *Mater. Chem. Phys.*, 114 (2009) 533.
24. H.H. Abdel-Rahman, A.M. Ahmed, A.A. Harfoush, A.H.E. Moustafa, *Hydrometallurgy*, 104 (2010) 169.
25. Y.K. Agrawal, J.D. Talati, M.D. Shah, *Corros. Sci.*, 46 (2004) 633.
26. Y. Nuhoglu, E. Malkoc, *Bioresource Tech.*, 100 (2009) 2375.
27. E.E. Ebenso, *Bull. Electrochem.*, 19 (2003) 209.
28. S. Sathiyarayanan, C. Jeyaprabha, S. Muralidharan G. Venkatachari, *Appl. Surf. Sci.*, 252 (2006) 8107.
29. V. T. Truong, P. K. Lai, B. T. Moore, R. F. Muscat, M. S. Russo, *Synth. Met.*, 110 (2000) 7.
30. U. Rammelt, P. T. Nguyen, W. Plieth, *Electrochim. Acta*, 48 (2003) 1257.
31. I.E. Selim, A.m. Ahmed, A.A. Khedr, H.M.A. Soliman, *Bull. Electrochem.*, 17 (2001) 27.
32. N.D. Nikolic, G. Brankovic, M.G. Pavlovic, and K.I. Popov, *Electroanal. Chem.*, 621 (2008) 13.
33. N.D. Nikolic, K.I. Popov, Lj.J. Pavlovic, M.G. Pavlovic, *Powder Technol.*, 185 (2008) 195.
34. G. Wranglen, *Electrochim. Acta*, 2 (1960) 130.
35. N.D. Nikolic, K.I. Popov, Lj.J. Pavlovic, M.G. Pavlovic, *Surf. Coat. Technol.*, 201 (2006) 560.
36. H.- C. Shin, J. Dong, M. Liu, *Adv. Mater.*, 15 (2003) 1610.
37. T.A. Witten, and L.M. Sander, *Phys. Rev. Lett.*, 47 (1981) 1400.
38. D.G. Offen, P.R. Birkin, T.G. Leighton, *Electrochem. Commun.*, 9 (2007) 1062.
39. A. Ciszewski, S. Posluszny, G. Milczarek, M. Baraniak, *Surf. Coat. Technol.*, 183 (2004) 127.
40. G. Yue, X. Lu, Y. Zhu, X. Zhang, S. Zhang, *Chem. Eng.*, 147 (2009) 79.
41. P. Sahoo, *Mater. Des.*, 30 (2009) 1341.
42. M. M. Abou-Krishna, *Appl. Surf. Sci.*, 252 (2005) 1035.

43. T. Borkar, S. Harimkar, *Surf. Coat. Technol.*, 205 (2011) 4124.
44. M. Hosseini, S. Ebrahimi, *Electroanal. Chem.*, 645 (2020) 109.

© 2012 by ESG (www.electrochemsci.org)